Journal of Materials Chemistry C

Accepted Manuscript

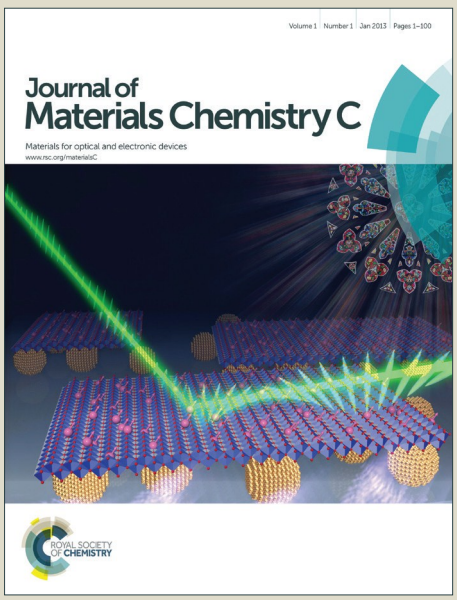

ROYAL SOCIETY OF CHEMISTRY

www.rsc.org/materialsC

Journal Name

ARTICLE

Highly stretchable and sensitive strain sensor based on graphene-elastomer composites with a novel double-interconnected network

Received 00th January 20xx,
Accepted 00th January 20xx

DOI: 10.1039/x0xx00000x

www.rsc.org/

Yong Lin, Shuqi Liu, Song Chen, Yong Wei, Xuchu Dong, Lan Liu*

The construction of a continuous conductive network with a low percolation threshold plays a key role in fabricating a high performance strain sensor. Herein, a highly stretchable and sensitive strain sensor based on binary rubber blend/graphene was fabricated by a simple and effective assembly approach. A novel double-interconnected network composed of compactly continuous graphene conductive networks, was designed and constructed in the composites, thereby resulting in an ultralow percolation threshold of 0.3 vol%, approximately 12-fold lower than that of the conventional graphene-based composites with a homogeneously dispersed morphology (4.0 vol%). Near the percolation threshold, the sensors could be stretched in excess of 100% applied strain, and exhibited a high stretchability, sensitivity (gauge factor ~82.5) and good reproducibility (~300 cycles) of up to 100% strain under cyclic tensile tests. The proposed strategy provides a novel effective approach for constructing a double-interconnected conductive network in polymer composites, and exhibits very competitive for developing and designing high performance strain sensors.

Strain sensors based on the electrical signals (*e.g.* capacitance, resistance.) upon mechanical deformations have recently aroused considerable attention because of their potential application in wearable electronics[1,2], health monitoring[3,4], and human motion detection[5,6], *etc*. Even though the traditional strain sensors based on metallic and semiconducting materials possesses a high sensitivity (~10^3 of gauge factor), they are not capable for application in specific fields due to their poor stretchability (~5%).[7,8] To date, various approaches have been proposed to fabricate the highly stretchable and sensitive strain sensors based on conductive elastomer composites containing nanomaterials (*e.g.* silver nanowires[9], carbon nanotubes (CNTs)[10], graphene (GE)[11], *etc*). Wang *et al.*[12] reported the fabrication of the nanohybrids network based on CNTs and cellulose nanocrystals (CNCs), and then serving as a 3D hierarchical conductive structure in elastomer matrix to obtain a highly stretchable and sensitive sensor. However, such exposed drawback for most of these previously reported sensors is that they usually required rather high filler content (namely, high percolation threshold) for achieving satisfactory electrical properties, which results in a poor sensitivity, flexibility, mechanical performances, and high cost. Besides, these sensors required complicated processes that are unsuitable for practical applications. To further address these issues, constructing a conductive network with a low percolation threshold is a promising and effective approach to fabricate a highly flexible, stretchable and sensitive strain sensor.

More recently, the utilization of GE as an electrically conductive filler in composites shows significant potential for strain sensor applications[13-15] because of its remarkable electrical and mechanical performance[16,17]. As comparison to other conductive nanomaterials (*e.g.* CNTs, carbon black (CB)), GE can remarkably endue the elastomer composites with outstanding conductivity at a lower content. Nowadays, it has been found that constructing a continuous interconnected GE networks in polymer matrix can serve as an effective strategy for fabricating the GE-based conductive polymer composites with a low percolation threshold[18-20]. For example, Xia *et al.*[21] reported a latex assembly technique to prepare high performance conductive rubber composites with an interconnected network, and a low percolation threshold of 0.62 vol% was achieved. Also, Lin *et al.*[22] presented a novel pre-construction method to fabricate conductive rubber composites with a three dimensional conductive GE network, exhibiting a percolation threshold of 0.55 vol%. Although such interconnected networks have been constructed by several approaches, a rather high conducting percolation threshold is usually necessary for showcasing unsatisfied electrical properties for these conductive elastomer composites by constructing an effective conductive network throughout the whole matrix, resulting in a severe damage to mechanical properties of composites. Also, those conductive composites display a limited potential, because of their relatively complicated process and high-cost production. Therefore, the challenge lies in designing and constructing, by means of a simple and effective process, a novel interconnected GE channel in elastomer matrix.

College of Materials Science and Engineering, Key Lab of Guangdong Province for High Property and Functional polymer Materials, South China University of Technology, Guangzhou 510641, PR China.
E–mail: psliulan@scut.edu.cn
† Electronic Supplementary Information (ESI) available: supplementary information is available free of charge via the Internet at http://pubs.rsc.org/. See DOI: 10.1039/x0xx00000x

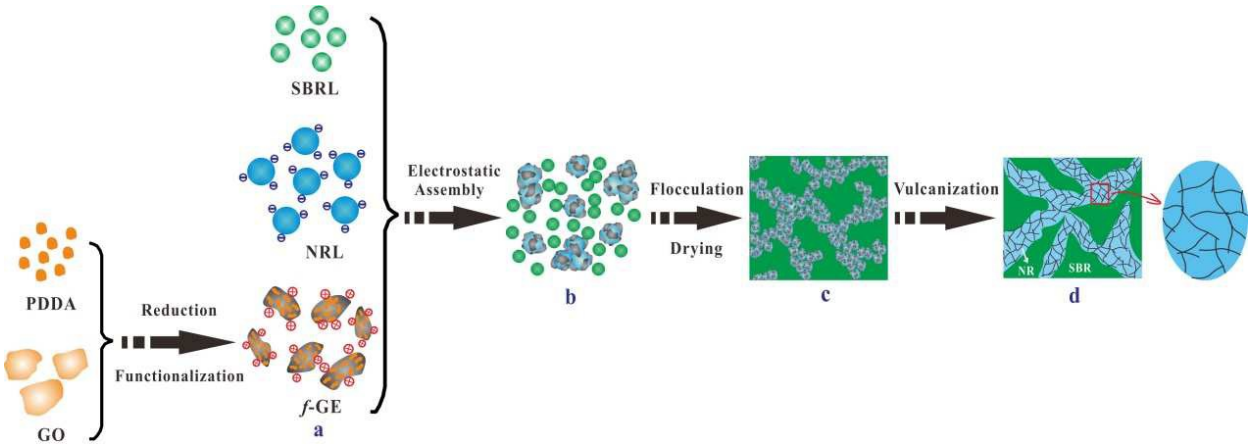

Scheme 1 Schematic illustration for the fabrication of SBR/NR-GE with a double-interconnected network.

Here, we developed highly stretchable and sensitive strain sensor based on a simple and effective assembly approach, which endowed a conductive butadiene styrene rubber (SBR)/natural rubber (NR) composites with a novel conductive network. The assembly process driven by electrostatic interactions between functionalized graphene (*f*-GE, positively charged) and NR latex particles (negatively charged) conduces to the interconnected NR/GE channels. Then the double-interconnected conductive networks were formed from the percolated NR/GE channels with an intact interconnected structure: the NR/GE channels were localized at the interface between the SBR phases, forming another interconnected structure. Different from the segregated GE structures in polymer matrix reported by Xia *et al.*[21], Lin *et al.*[22], *etc*, the constructed double-interconnected network fabricated by our approach can result in more compactly continuous and narrow conductive channels at a extremely low GE content, instead of being interconnected throughout the whole matrix at high GE content, consequently, such network structure realized a much lower percolation threshold for the conductive composites. Depending on the double-interconnected network structures, the fabricated strain sensors exhibited high stretchability (up to 120%), good sensitivity (gauge factor, ~82.5) and reproducibility (~300 stretching/releasing cycles) even when strained up to 100%, which tremendously provide the basis for practical strain sensor applications. To the best of our knowledge, there is no prior report on the construction of a novel double-interconnected network in rubber composites. Additionally, our approach to fabricate a double-interconnected network in rubber matrix is simple, low-cost and scalable, which can be easily modulated to accommodate other elastomer systems (*e.g.* NR/nitrile butadiene rubber (NBR), NR/butadiene rubber (BR), *etc*.).

The assembly approach for fabricating SBR/NR composites with a double-interconnected conductive network is schematically illustrated in Scheme 1. Firstly, PDDA was introduced to tailor the GE surface for preparing *f*-GE with a positively charge (Scheme 1a), and the functionalization of GE was clearly verified by the FT-IR, UV-vis and TGA analysis, as shown in Fig. S2. Then *f*-GE was subjected into the mixture of NR latex (NRL) and SBR latex (SBRL). The strong electrostatic attraction between *f*-GE (positively charged) and NRL particles (negatively charged) served as the driving force for the assembly process (Scheme 1b), further confirmed by zeta potential measurement in Fig. S3. Also, TEM observations provide visual evidence for the proposed assembly. *f*-GE compactly encapsulated NRL particles are clearly observed in Fig. S4. Next, the mixed latex was coagulated and filtrated (Scheme 1c). Finally, the composites with a double-interconnected conductive network were obtained using hot compression (Scheme 1d). Note that the experimental details for the materials, preparation, and characterizations are detailedly described in the Supporting Information.

We first observed the morphology of the SBR/NR-GE composites as shown in Fig. 1. Expectedly, a double-interconnected network is effectively constructed, where NR/GE conductive channels are located at the interfaces of SBR phase to form a compactly interconnected structure (Fig. 1a,b), while the NR/GE conductive channels themselves also are composed from another compactly interconnected GE network in the NR phase (see the higher magnified TEM image in Fig. 1b). A comparison of the TEM microphotographs for SBR/NR/GE are provided in Fig. 1c,d, and it clearly presents the random distribution of GE in the homogeneous blends, instead of being compactly interconnected throughout the whole SBR/NR/GE matrix. It is worth noting that these observations very coincide with the SEM results (Fig. S5).

In order to further verify the double-interconnected network, the cryo-fractured SBR/NR-GE was etched with toluene for 3 h to remove the matrix, and the morphologies of the extracted GE skeleton for the un-vulcanized samples were observed by SEM as shown in Fig. 2. It is evident in Fig. 2a,b that a continuous, interconnected network skeleton exists throughout the matrix, which is consistent with the TEM observation in the Fig. 1b. As a comparison, the extracted morphology shown in Fig 2c,d indicates that SBR/NR/GE have a homogeneously dispersed morphology, and the continuous GE network structure is not constructed with the inclusion of the addition of the non-functionalized GE. It is believed that such different morphologies will directly result in the distinct performance of composites.

To evaluate the effect of different morphologies on the performance of composites, the electrical conductivity and mechanical performances of SBR/NR-GE and SBR/NR/GE as a

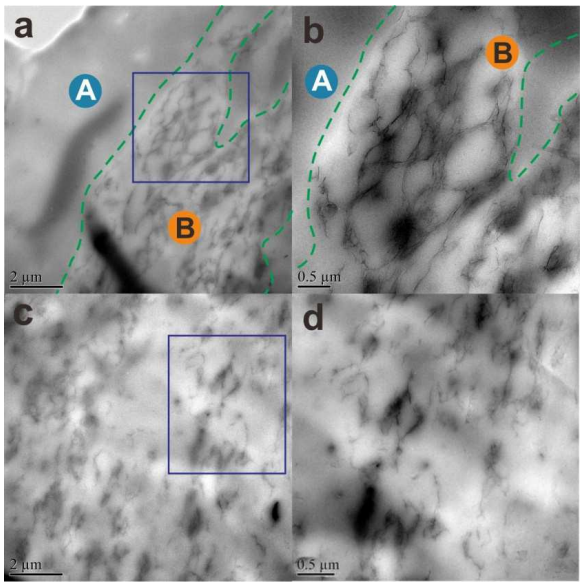

Fig. 1 TEM images of SBR/NR-GE-0.42 (a and b), and SBR/NR/GE-0.42 (c and d). Region A corresponds to the SBR phase and region B represents the NR phase containing *f*-GE.

function of GE content were investigated. As shown in Fig. 3a, a very lower conductive *f*-GE content endows the composites with higher conductivity as compared with GE. With 0.42 vol% of *f*-GE, the conductivity of the double-interconnected SBR/NR-GE reaches ~1.04×10^{-5} S/m. However, for the SBR/NR/GE with the same content of GE, its conductivity is only ~5.20×10^{-10} S/m, which is nearly 5 orders of magnitude lower than that of SBR/NR-GE. Such phenomenon demonstrates the high efficiency of the double-interconnected network in forming the electrically conductive paths.

For further analyzing the relationship between filler content and electrical conductivity of composites, a power law equation is used to compute the electrical percolation threshold (φ_c).[23]

$$\sigma=\sigma_0(\varphi-\varphi_c)^t$$

where σ and σ_0 are the electrical conductivity of the composites and the proportionality constant assigned to the intrinsic conductivity of the filler, respectively. φ is the volume fraction of the fillers and φ_c is the percolation volume fraction, and t represents the critical exponent.

The double-logarithmic plot of electrical conductivity versus (φ-φ_c) is displayed in Fig. 3b. Specifically, φ_c values are 0.3 and 4.0 vol%, the values of t were 4.83 and 1.62 for SBR/NR-GE and SBR/NR/GE, respectively. Notably, the percolation threshold of SBR/NR-GE is ~12-fold lower than that of SBR/NR/GE. Such low percolation threshold is attributable to the construction of double-interconnected conductive network in the matrix. Specifically, this phenomenon can be interpreted as follows. A strong electrostatic attraction interaction effectively facilitate the formation of *f*-GE compactly encapsulated NRL particles, further providing a precondition for the construction of a compactly interconnected GE network in the NR phase. Moreover, a volume-extrusion effect originated from the SBR phases greatly exerts a force for constructing another interconnected NR/GE network throughout

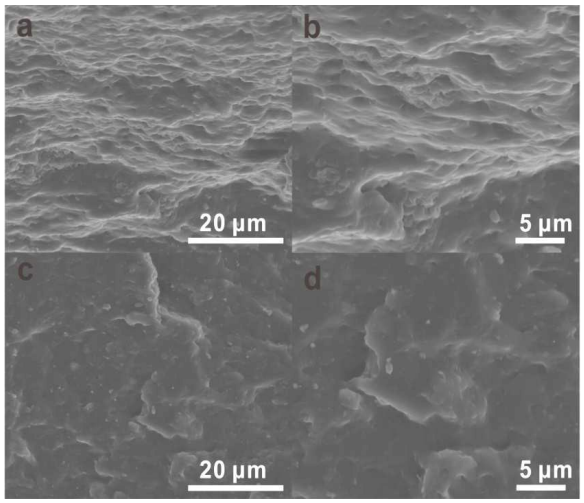

Fig. 2 SEM images of the extracted conductive network skeleton for the un-vulcanized SBR/NR-GE-0.42 (a and b) and SBR/NR/GE-0.42 (c and d).

the SBR/NR blend. These results efficiently promote the construction of a compactly double-interconnected network. Noteworthily, in view of the balance of the percolation threshold and the corresponding electrical conductivity, one can be reasonably concluded that the electrical behaviour of our composites is very superior to those reported for NR/GE[24], PDMS/GE[25], TPU/GE [26], ENR/GE[27], *etc*, and a more detailed comparison is tabulated in Table S2.

It has been reported in general that the critical exponent t is largely dependent on the dimensionality of composites, further interpret the polymer-fillers network structure in the composites. It was proposed that t < 2.1 suggests the polymer matrix with a bridged polymer-filler network, whereas t > 3.75 indicates the construction of filler-filler interconnected networks in the polymer matrix. Therefore, a t value of 1.62 for SBR/NR/GE is indicative of the establishment of a bridged polymer-GE network. Also, a t value of 4.83 for SBR/NR-GE manifests the existence of interconnected GE networks in the matrix. In addition, as shown in Fig. S6, the enhancements of the elastic modulus (G′) and torque (M) for the SBR/NR-GE are much higher than those for the SBR/NR/GE composites. Obviously, G′ and M of SBR/NR-GE-1.66 are very close to those of SBR/NR/GE-3.27. This is a further indicative of the formation of a more developed interconnected GE network and a stronger interfacial interaction in the SBR/NR-GE. As a result, it is reasonably concluded that the constructed double-interconnected network can serve to significantly reduce the percolation threshold and enhance the electrical conductivity of the composites.

Furthermore, a comparison of mechanical properties of SBR/NR-GE and SBR/NR/GE as a function of GE content was employed. Hereon, we chose SBR/NR-GE and SBR/NR/GE-0, 0.42, 0.84, 1.66, 3.67 and SBR/NR/GE-0, 0.42, 0.84, 1.66, 3.67 with no, relatively low or high content of GE to analyze the mechanical properties. Fig. S7(a,b) computes the modulus at 300% strain and tensile strength of SBR/NR composites with and without double-interconnected structures at different GE contents. And Fig. S7(c) shows the representative uniaxial tensile stress-strain curves of the

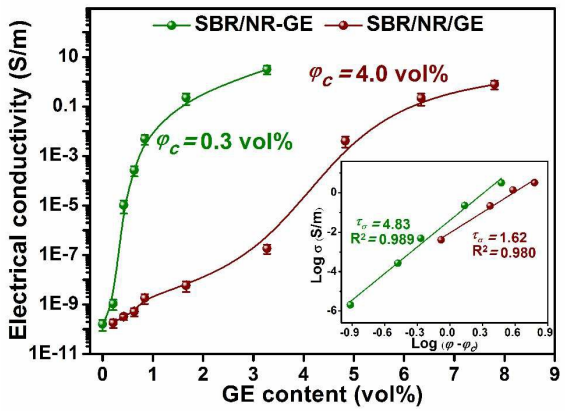

Fig. 3 Electrical conductivity of SBR/NR composites as a function of GE content. The inset is the fitted results of experimental data of SBR/NR-GE and SBR/NR/GE according to the percolation law.

composites. It can be seen that the modulus at 300% strain for SBR/NR-GE showed significantly higher value, when compared with SBR/NR/GE with the same content of GE. It is also be observed that the tensile strength of the SBR/NR-GE always maintains the similar level as the SBR/NR/GE with the same content of GE, showing maintained tensile flexibility of SBR/NR-GE composites. Such enhanced mechanical performances for the SBR/NR-GE samples can be attributed to the effect of the constructed double-interconnected GE network, which serves to the efficient reinforced networks toward rubber matrix. This hierarchical interconnected network throughout the matrix is conductive to dissipating a large amount of energy through the interconnected interface, effectively withstanding the external loading, and thus endowing the SBR/NR-GE with comparable mechanical properties. Noteworthily, the strong interfacial interaction between the interconnected GE network and the matrix plays a role in the improvement of mechanical performance, strongly evidenced by the analysis based on the well-known Mooney-Rivlin equation, as shown in Fig. S7(d).

For practical applications, the elasticity of the composites should be required to investigate. As reported, the elasticity can be tested from the tensile extension-relaxation measurements, detailedly reflected by the elastic recovery (ER_ε), as calculated in the following equation[28].

$$ER_\varepsilon = \frac{\varepsilon - \varepsilon_R}{\varepsilon} \times 100$$

where ε is the applied strain, and ε_R is the residual strain after extension-relaxation tests. The representative extension-relaxation curves are displayed in Fig. S8(a,b) and the results are shown in Fig. S8(c). The total elastic recovery of SBR/NR-GE samples is more than 75% after 300% strain. Evidently, SBR/NR-GE exhibit more superior ER_ε as a comparison of SBR/NR/GE, revealing the excellent elasticity of composites with such a developed interconnected network. Noteworthily, The Shore A hardness of all SBR/NR-GE and SBR/NR/GE are also tested and the results can be seen in Fig. S8(d). The Shore A hardness of SBR/NR-GE is significantly lower than those of SBR/NR/GE with the same content of GE, suggesting much better elasticity of SBR/NR-GE. This behaviour is mainly attributed to that the selective distribution of *f*-GE in NR phase has a negative effect on mechanical rigidity. Therefore, these results demonstrate that the double-interconnected conductive GE network plays an important role in effectively reducing the percolation threshold and enhancing mechanical performance of composites.

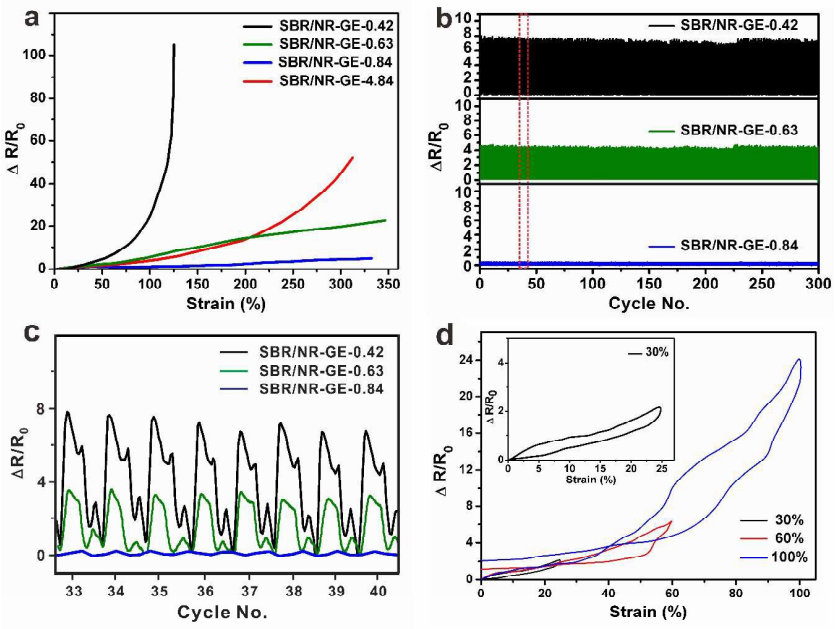

Fig. 4 (a) Plot of the $\Delta R/R_0$ as a function of applied strain. (b) Plot of the $\Delta R/R_0$ under 300 stretching/releasing cycles of 30%. (c) Plot of the $\Delta R/R_0$ for cycles 33-40. (d) Hysteresis curve for the strain sensors. The inset in (d) shows the enlarged image of hysteresis curve for SBR/NR-GE-0.42 when stretched to 30% strain levels.

Journal Name

ARTICLE

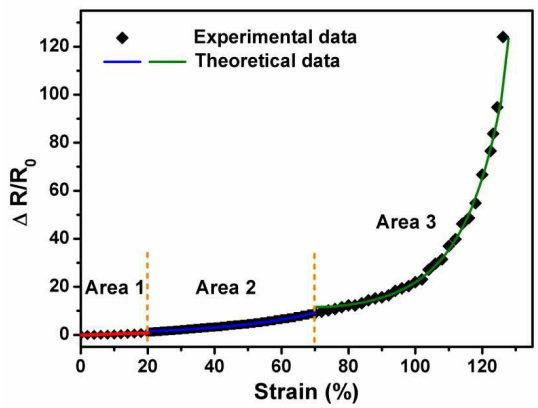

Fig. 5 Experimental (dots) and theoretical (solid lines) data of $\Delta R/R_0$ as a function of strain in different strain amplitude.

Furthermore, the prepared SBR/NR-GE with a double-interconnected conductive network simultaneously possesses the superior mechanical flexibility, high electrical conductivity and low percolation threshold, which makes it competitive as flexible sensing material. The effect of GE content on the strain sensing behaviour of composites was then investigated. Fig. 4a shows the relative resistance change ($\Delta R/R_0$) of the SBR/NR composites as a function of strain at a strain rate of 4 min^{-1}. The relative resistance change ($\Delta R/R_0$) is defined as the ratio of the resistance change (ΔR) to the resistance (R_0) at the initial state. It is evident that the sensitivity of $\Delta R/R_0$ for SBR/NR-GE is very dependent on the applied strain. As can be seen, the curve for SBR/NR-GE-0.42 can be divided into three different regions with 20%, 70% strain as division points.

The main reason for the different changed regions is thought to be the evolution of the double-interconnected conductive network resulting from the deformation of the rubber matrix. Fig. 5 shows the measured strain-dependent relatively resistance change $\Delta R/R_0$ of SBR/NR-GE-0.42. When the composites are stretched below 20% strain (area 1), the percolated NR/GE channels with an interconnected structure is stretched as a priority at this stage, in which the very weak wriggle of the GE sheets and the extrusion effect originated from the SBR phases have trifling impact on the evolution of internal interconnected GE network structures in the NR phase. So a very weak resistance change is observed in the composites at small strain (below 20%). As the further strain is applied below 70% strain (area 2), the $\Delta R/R_0$ has a relatively gentle increase, whereas a sharp rise in $\Delta R/R_0$ is a distinct tendency above 70% strain (area 3). This different change can be attributed to the evolution of the interconnected GE network in the NR phase at higher strain. Herein, a model based on tunneling theory is proposed to explain the above-observed experimental results. The total electrical resistance R of the composite can be calculated as equation 1[29]:

$$R = (\frac{L}{N})(\frac{8\pi hs}{3\gamma a^2 e^2})\exp(\gamma s) \quad (1)$$

where N is the number of conducting paths, L is the number of particles forming a single conducting path, a^2 is the effective cross section, e is the electron charge, h is the Plank constant, s is the smallest distance between conductive particles. Here, γ is calculated as equation 2:

$$\gamma = \frac{4\pi}{h}\sqrt{2\varphi m} \quad (2)$$

where φ is the height of the potential barrier between adjacent particles, m is the electron mass.

When an external stress is applied towards the composites, the resistance change can be caught due to the particles separation in the matrix. Assuming that the particle separation proportionally varies from s_0 to s under the applied strain, and the number of conducting paths decreases from N_0 to N, the separation s, conducting paths N and relative resistance ($\Delta R/R_0$) can be expressed as eqns 3, 4 and 5, respectively.

$$s = s_0(1 + b\varepsilon) \quad (3)$$

$$N = \frac{N_0}{\exp[A_1\varepsilon + B]} \quad (4)$$

$$\frac{\Delta R}{R_0} = \frac{R - R_0}{R_0} = (\frac{Ns}{N_0 s_0})\exp[\gamma(s - s_0)] - 1 \quad (5)$$

where b is the constant, s_0 is the initial particle separation, ε is the tensile strain of the rubber matrix, N_0 is the initial number of conducting path, A and B are constants, R_0 is the initial resistance, and ΔR is the resistance change under the tensile strain.

The substitution of eqn (3) and (4) into equation (5) yields:

$$\frac{\Delta R}{R_0} = (1 + \varepsilon)\exp[A\varepsilon + C] \quad (6)$$

where $A = A_1 + \gamma s$. The experimental data shown in area 2 is compared to equation 6 and the result is shown in Fig. 5. A good agreement between the experimental curve and theoretical curve is achieved at A= 4.5837 and C= -0.9282 for area 2.

Noteworthily, in area 3 of the curve, a higher increase rate of $\Delta R/R_0$ at higher strain is clearly observed, which may be attributable of the severe destruction of the conductive GE network in the matrix. It is also conceivable that a much smaller number of conducting paths N will be formed at higher tensile strain, further expressed by the following equation 7.

$$N = \frac{N_0}{\exp[A_2\varepsilon + B\varepsilon^2]} \quad (7)$$

where A_2 and B are constants. The substitution of eqns 3 and 7 into equation 6 yields:

$$\frac{\Delta R}{R_0} = (1 + \varepsilon)\exp[A\varepsilon + B\varepsilon^2] \quad (8)$$

Journal Name

ARTICLE

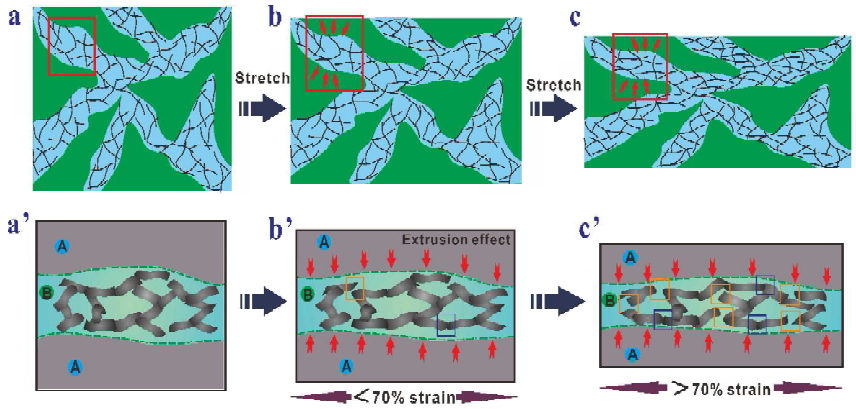

Fig. 6 Schematic illustration for the evolution of conductive network in a stretching process. (a) The original state; (b) the stretching state lower to 70% strain; and (c) the stretching state up to 70% strain. Region A corresponds to the SBR phase and region B represents the NR phase containing *f*-GE. Thereinto, (a'), (b') and (c') are corresponding to the magnified regions in the (a), (b) and (c), respectively.

where $A = A_2 + \gamma s$. The experimental data for the area 3 under high strain are fitted with equation 8 and are also shown in Fig. 5. Notably, equation 8 derived from tunneling theory, well describes the experimental data with A= 1.9070 and B= 0.6405 for area 3.

Thus, the experimental results over the 20% strain ranges can be fitted well using the tunneling conduction model, which suggests that the tunneling theory plays a dominant role in for transporting charge carriers in the composites. Importantly, we therefore believe that the constructed double-interconnected network is responsible for the difference in the resistance-strain sensing behaviour.

To better understand the observed phenomenon in area 2 and area 3, a mechanism about the evolution of double-interconnected conductive networks in a stretching process is illustrated in the Fig. 6. In the original state (Fig. 6a,a'), the interconnected GE network is very compact. When the samples are stretched in area 2 (Fig. 6b,b'), the breakage of conductive networks (appearing as orange rectangle) can be occurred due to the movement of NR chains and the extrusion effect originated from the SBR phase, leading to the disruption of the interconnected points between GE sheets. Synchronously, some conductive networks (appearing as blue rectangle) are reconstructed. The destruction and reconstruction of the conductive GE network coexist in the stretching process. When the destruction of conductive networks significantly dominates, the $\Delta R/R_0$ exhibits an increase. However, the application of further tensile strain (above 70%) will give rise to the decrease of abundant contact junctions by breaking the conductive pathways, leading to a sudden increase in electrical resistance. Notably, in the releasing process, some interconnected points between GE sheets are reconstructed, resulting in an effective conductive network, whereas the irreversible destruction of conductive GE network also exists in the composites, causing an irreversible resistance. It should be noted that the applied strain amplitude greatly affected the irreversible phenomenon. In Fig. 4d, the $\Delta R/R_0$ of SBR/NR-GE-0.42 is nearly recovered for stretching/releasing cycles with 60, 100% strain. Moreover, a highly reversible change in $\Delta R/R_0$ can be obviously observed in the cyclic tests cycles with 30% strain.

Besides, the gauge factor $[\Delta R/(\varepsilon R_0]$ of the sensors is calculated in order to reflect the sensitivity of the sensor to strain. The sensitivity of sensor has a positive correlation with the gauge factor. As can be seen from Fig. 4a, the gauge factor of SBR/NR-GE-0.42 is estimated to be ~82.5 with a high stretchability of ~100% strain. Delightedly, the gauge factor of the SBR/NR-GE are very competitive to those of strain sensor materials based on the nanomaterials of CB, CNT and GE previously reported[25,30-34], and a more detailed comparison is tabulated in Table S3. Such result demonstrates that the SBR/NR-GE with low GE concentrations just above the percolation threshold exhibits very competitive for fabricating the highly flexible and sensitive strain sensors under some special conditions.

To verify the durability and reproducibility of the strain sensor after repetitive cyclic stretching/releasing, the fabricated sensors were measured after repetitive stretching of 300 cycles up to 30% strain. During the cyclic tests as shown in Fig. 4b and c, the sensors after cyclic stretching/releasing still maintain an electrical performance (high stability and high sensitivity) similar to that before the cyclic stretching tests, showing a good recoverability and reproducibility. In a closer view of resistance-strain behaviour in Fig. 4c, as for SBR/NR-GE-0.42 and SBR/NR-GE-0.63, an apparent 'shoulder peak' appears during the cyclic loading, phenomenon of which has also been observed in the TPU/GE[26] and polymer/CNT[35], *etc*. It is believed that such phenomenon is closely related to the destruction and reconstruction of the conductive network during the stretching/releasing process. As a comparison, the 'shoulder peak' is not observed for SBR/NR-GE-0.84, and the $\Delta R/R_0$ exhibits a much flat response to cyclic loading. At the GE concentrations much

above the percolation threshold (0.84 vol%), a much compactly interconnected conductive GE network throughout the composites is constructed, which is beneficial to avoid the damage of conductive paths and leads to a better conductive network under the re-construction the GE network with a strain of more than 300%.

Therefore, the fabricated strain sensors exhibit high stretchability, and good sensitivity over a wide tensile strain range and possess good recoverability and reproducibility after stabilization by cyclic stretching, indicating a unique strain reversible electric response upon application of tensile strain. In view of the competitive and promising strain sensing performance, the conductive SBR/NR-GE composites with a novel double-interconnected network have great potential for applications as strain sensors to meet various demands in stretchable electronics, skin sensors, wearable communication devices, *etc*.

Conclusions

We reported a simple, facile assembly approach to prepare highly stretchable and sensitive strain sensors with a novel double-interconnected conductive network. The construction of a double-interconnected GE network significantly enhanced the electrical properties and reduced the electrical percolation threshold of the composites. The percolation threshold of the SBR/NR-GE with the double-interconnected network structures was 12-fold lower than that of the SBR/NR/GE with homogeneous dispersion morphology. Moreover, the fabricated strain sensors exhibited good stretchability, sensitivity (gauge factor, ~82.5) and reproducibility (~300 cycles) even when strained up to 100%, which makes it suitable for human body motion detection under large strain. The strong assembly driven by electrostatic interactions between *f*-GE and NRL particles and the volume-extrusion effect originated from the SBR phases conduced to the construction of a compactly double-interconnected GE network, thus enabling the strain sensors with the excellent performances. Such properties can pave the way for potential applications of the strain sensor based on GE-elastomer composites in stretchable electronics, physical motion detection, and other related areas.

Acknowledgements

This work is financially supported by National Basic Research Program of China (No. 2015CB654700 (2015CB654703)), National Natural Science Foundation of China (No. 51573053) and Science and Technology Planning Project of Guangdong Province (No. 2014A010105022).

Notes and references

1 M. Amjadi, M. Turan, C. P. Clementson and M. Sitti, *ACS Appl. Mater. Interfaces*, 2016, **8**, 5618.
2 J.-Y. Jeon and T.-J. Ha, *ACS Appl. Mater. Interfaces*, 2016, **8**, 2866.
3 I. Kang, M. J. Schulz, J. H. Kim, V. Shanov and D. A. Shi, *Smart Mater. Struct.*, 2006, **15**, 737.
4 C. Hung, S. K. Thakar, M. L. Oseng, C. M. Nguyen, C. Jebali, A. B. Kouki and J.-C. Chiao, *IEEE Sens. J.*, 2015, **15**, 6542.
5 B. C. Zhang, H. Wang, Y. Zhao, F. Li, X. M. Ou, B. Q. Sun and X. H. Zhang, *Nanoscale*, 2016, **8**, 2123.
6 S. Ryu, P. Lee, J. B. Chou, R. Xu, R. Zhao, A. J. Hart and S.-G. Kim, *ACS Nano*, 2015, **9**, 5929.
7 Y. Kim, Y. Kim, C. Lee and S. Kwon, *IEEE Sens. J.*, 2010, **10**, 1320.
8 J. C. F. Millett, N. K. Bourne and Z. Rosenberg , *J. Phys. D: Appl. Phys.*, 1996, **29**, 2466.
9 M. Amjadi, A. Pichitpajongkit, S. Lee, S. Ryu and I. Park, *ACS Nano*, 2014, **8**, 5154.
10 R. Rahimi, M. Ochoa, W. Y. Yu and B. Ziaie, *ACS Appl. Mater. Interfaces*, 2015, **7**, 4463.
11 S.-H. Bae, Y. Lee, B. K. Sharma, H.-J. Lee, J.-H. Kim and J.-H. Ahn, *Carbon*, 2013, **51**, 236.
12 S. Wang, X. Zhang, X. Wu and C. Lu, *Soft Matter*, 2016, **12**, 845.
13 J. W. Zha, B. Zhang, R. K. Y. Li and Z. M. Dang, *Compos. Sci. Technol.*, 2016, **123**, 32.
14 Y. Wang, L. Wang, T. Yang, X. Li, X. Zang, M. Zhu, K. Wang, D. Wu and H. Zhu, *Adv. Funct. Mater.*, 2014, **24**, 4666.
15 J. D. Shi, X. M. Li, H. Y. Cheng, Z. J. Liu, L. Y. Zhao, T. T. Yang, Z. H. Dai, Z. G. Cheng, E. Z. Shi, L. Yang, Z. Zhang, A. Y. Cao, H. W. Zhu and Y. Fang, *Adv. Funct. Mater.*, 2016, **26**, 2078.
16 A. K. Geim and K. S. Novoselov, *Nat. Mater.*, 2007, **6**, 183.
17 C. Lee, X. Wei, J. W. Kysar and J. Hone, *Science*, 2008, **321**, 385.
18 J. R. Potts, O. Shankar, L. Du and R. S. Ruoff, *Macromolecules*, 2012, **45**, 6045.
19 H. Pang, L. Xu, D. X. Yan and Z. M. Li, *Prog. Polym. Sci.*, 2014, **39**, 1908.
20 Y. Y. Luo, P. F. Zhao, Q. Yang, D. N. He, L. X. Kong and Z. Peng, *Compos. Sci. Technol.*, 2014, **100**, 143.
21 Y. H. Zhan, M. Lavorgna, G. Buonocore and H. S. Xia, *J. Mater. Chem.*, 2012, **22**, 10464.
22 Y. Lin, S. Q. Liu and L. Liu, *J. Mater. Chem. C*, 2016, **4**, 2353.
23 J.-C. Huang, *Adv. Polym. Technol.*, 2002, **21**, 299.
24 Y. Y. Luo, P. F. Zhao, Q. Yang, D. N. He, L. X. Kong and Z. Peng, *Compos. Sci. Technol.*, 2014, **100**, 143.
25 S.-H. Bae, Y. Lee, B. K. Sharma, H.-J. Lee, J.-H. Kim and J.-H. Ahn, *Carbon*, 2013, **51**, 236.
26 H. Liu, Y. L. Li, K. Dai, G. Q. Zheng, C. T. Liu, C. Y. Shen, X. R. Yan, J. Guo and Z. H. Guo, *J. Mater. Chem. C*, 2016, **4**, 157.
27 C. Z. He, X. D. She, Z. Peng, J. P. Zhong, S. Q. Liao, W. Gong, J. H. Liao and L. X. Kong, *Phys. Chem. Chem. Phys.*, 2015, **17**, 12175.
28 M. Z. Seyedin, J. M. Razal, P. C. Innis, R. Jalili and G. G. Wallace, *Adv. Funct. Mater.*, 2015, **25**, 94.
29 X. W. Zhang, Y. Pan, Q. Zheng and X. S. Yi, *J. Polym. Sci. Part B: Polym. Phys.*, 2000, **38**, 2739.
30 S. M. Wang, X. X. Zhang, X. D. Wu and C. H. Lu, *Soft Matter*, 2016, **12**, 845.
31 C. Mattmann, F. Clemens and G. Trőster, *Sensors*, 2008, **8**, 3719.
32 C. S. Boland, U. Khan, C. Backes, A. O'Neill, J. McCauley, S. Duane, R. Shanker, Y. Liu, I. Jurewicz and A. B. Dalton, *ACS Nano*, 2014, **8**, 8819.
33 P. Slobodian, P. Riha, R. Benlikaya, P. Svoboda and D. Petras, *IEEE Sens. J.*, 2013, **13**, 4045.
34 N. Lu, C. Lu, S. Yang and J. Rogers, *Adv. Funct. Mater.*, 2012, **22**, 4044.
35 J. Du, L. Zhao, Y. Zeng, L. Zhang, F. Li, P. Liu and C. Liu, *Carbon*, 2011, **49**, 1094.

Table of Contents

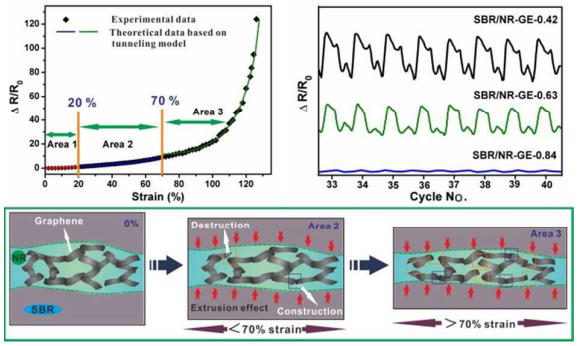

A facile assembly approach was firstly reported to fabricate a highly stretchable and sensitive strain sensor based on graphene-rubber composites with a novel double-interconnected network.